ELSEVIER

Polymer 43 (2002) 3611–3620

polymer

www.elsevier.com/locate/polymer

Kinetics of demixing and remixing in poly(ethylene oxide)/poly(ether sulphone) blends as studied by modulated temperature differential scanning calorimetry

Steven Swier, Ronny Pieters, Bruno Van Mele*

Department of Physical Chemistry and Polymer Science–FYSC (TW), Faculty of Applied Sciences, Vrije Universiteit Brussel (VUB), Pleinlaan 2, B-1050 Brussels, Belgium

Received 3 September 2001; accepted 22 February 2002

Abstract

The phase diagram of a poly(ethylene oxide)/poly(ether sulphone) blend is constructed using modulated temperature DSC and optical microscopy. It includes the glass transition (T_g), melting point (T_m) and cloud point temperature (T_{cl}), which define the regions of interest in this work: demixing above T_{cl}, followed by remixing in the miscible melt region between T_{cl} and T_m or T_g. The width of T_g has to be taken into account to understand partial vitrification effects during phase separation at high temperatures. Dynamic rheometry provides complementary information about partial vitrification and devitrification. Excess contributions due to demixing and remixing on the time-scale of the modulation appear in the heat capacity in both non-isothermal and quasi-isothermal conditions. This apparent heat capacity signal is used to study the effects of composition of the blend and molecular weight of the constituents on the demixing and remixing kinetics and on the interrelation between both. Partial vitrification during demixing is important in this respect. Step-wise quasi-isothermal measurements show a time-independent excess heat capacity in between T_{cl} and the interference of vitrification.

Keywords: Modulated temperature differential scanning calorimetry; Apparent heat capacity; Kinetics of demixing and remixing

1. Introduction

The final morphology of partially miscible polymer blends is determined by the imposed thermal treatment. In the case of binary blends of a crystallizable component poly(ethylene oxide) (PEO) and a high-T_g amorphous component poly(ether sulphone) (PES), a nano-structured morphology can be formed by combining both phase separation and crystallization in the same processing schedule [1]. This blend is characterized by a miscible melt region between the melting point temperature of PEO, around 60 °C, and the lower critical solution temperature (LCST), around 75 °C [2]. The crystallization rate of PEO starting from an initially homogeneous blend, decreases with the amount of PES and both secondary crystallization and recrystallization can occur [3,4]. Demixing for different temperature–time schedules, prior to crystallization of PEO, provides information about the composition and fraction of the co-existing phases during phase separation [1]. It was concluded that, upon phase separation, structure formation occurs rapidly, while the composition of the co-existing phases still changes, indicative for a spinodal decomposition mechanism [5]. Also the amount of remixing of a demixed blend can be followed indirectly in this way.

The added value of modulated temperature DSC (MTDSC) to study phase separation in PEO/PES blends has been shown recently [6]. The (modulus of the complex, specific) heat capacity, C_p (J g^{-1}K^{-1}) has proven to be very useful. It is calculated as

$$C_p = \frac{A_{HF}}{A_T \omega} \tag{1}$$

where A_{HF} is the amplitude of the cyclic heat flow (W g^{-1}) and $A_T\omega$ is the amplitude of the cyclic heating rate, with A_T the temperature modulation amplitude (K), ω the modulation angular frequency ($=2\Pi/p$), and p the modulation period (s). A complete description of the extraction of the heat capacity and other MTDSC signals (total heat flow, reversing heat flow, non-reversing heat flow and heat flow phase) can be found in the literature [7,8]. The (almost

* Corresponding author. Tel.: +32-2-629-32-88/76; fax: +32-2-629-32-78.

E-mail address: bvmele@vub.ac.be (B. Van Mele).

0032-3861/02/$ - see front matter
PII: S0032-3861(02)00177-5

quantitative) separation of a thermal transformation (appearing in the non-reversing heat flow) from the heat capacity (associated with the reversing heat flow) provides valuable in situ information for the study of material systems such as thermosetting systems [9] and slowly crystallizing polymers [10]. In the former system, the non-reversing heat flow contains the enthalpy of reaction and the heat capacity can be associated with chemo-rheological changes during cure. The slow crystallization advancement can still be determined from a decrease in heat capacity in the latter case.

This straightforward separation is not valid in the case of phase separation in PEO/PES blends, since both signals contain information about the heat effects associated with demixing and remixing processes. For this reason the heat capacity is referred to as 'apparent heat capacity', to distinguish it from the baseline or equilibrium heat capacity, based on thermodynamics [6]

$$C_p^{\mathrm{app}}(T,t) = C_p^{\mathrm{thermo}}(T) + C_p^{\mathrm{excess}}(T,t) \quad (2)$$

C_p^{app} consists of a temperature-dependent part, C_p^{thermo}, and a part that is also time-dependent and changing with the progress of the transformation, C_p^{excess}. Cloud point temperatures for different compositions, detected as the onset in the evolution of C_p^{app} (or as the appearance of C_p^{excess}), show the LCST-type demixing behavior of this blend. Moreover, beyond the cloud point, the temperature-induced demixing process can be followed via C_p^{app}, including effects due to the enthalpy of demixing and due to partial vitrification of a high-T_g co-existing phase.

Since the enthalpy of demixing is very small in PEO/PES (less than 2 J g^{-1}), only noise is detected in the non-reversing heat flow, while the heat capacity signal still contains valuable information. Note that detectable changes in C_p^{app} due to phase separation can be as small as 0.01 J g^{-1} K^{-1}.

The present paper will further focus on the phase separation process in the partially miscible PEO/PES blend, as measured by MTDSC via the temperature- and time-dependency of C_p^{app}. The effect of composition of the blend, molecular weight of PEO and partial vitrification of the PES-rich co-existing phase on the kinetics of demixing and remixing will be investigated.

2. Experimental

2.1. PEO/PES blend preparation

PEO with viscosity average molecular weights of 4000 and 20,000 g mol^{-1} from Fluka Chemie AG; 8000 and 300,000 g mol^{-1} from Aldrich, was blended with PES, from Aldrich, with a viscosity average molecular weight of 20,000 g mol^{-1}. A range of compositions was obtained by preparing 10% (wt/vol) solutions of both components in dimethylformamide and by removal of the solvent under vacuum at 60 °C. The blends were additionally dried overnight at a temperature just below the cloud point of the blend.

The glass transition temperature, T_g, and the increment in heat capacity at T_g, ΔC_p, of PES were measured ($T_{g,PES} = 223$ °C and $\Delta C_{p,PES} = 0.18$ J g^{-1} K^{-1}). Literature values were taken for PEO ($T_g = -67$ °C and $\Delta C_p = 0.88$ J g^{-1}K^{-1} [11]).

2.2. Optical microscopy

Cloud points were detected by measuring the light transmitted through thin samples (held between glass slides) in a Mettler Toledo FP82HT hot stage equipped with a photodetector. A Spectratech optical microscope was used with a magnification of 4. All samples were heated at a rate of 1 °C min^{-1} to reduce thermal lag in the sample and to allow comparison with MTDSC measurements at the same underlying heating rate. A nitrogen purge avoided degradation of PEO at higher temperatures. The onset of the decrease in the transmitted light intensity was chosen as the cloud point temperature.

2.3. Dynamic rheometry

Small angle shear measurements were performed in controlled strain mode (displacement of $\pm 10^{-4}$ rad) with a TA Instruments AR 1000-N rheometer, equipped with an extended temperature module. Disposable aluminum parallel plates with a diameter of 2 cm were used. Temperature scans were performed at a heating rate of 1 °C min^{-1} and an oscillation frequency of 1 Hz.

2.4. Modulated temperature differential scanning calorimetry

The MTDSC measurements were performed on a TA Instruments 2920 DSC with MDSC™ option and RCS cooling system. Helium was used as a purge gas (25 ml min^{-1}). Indium and cyclohexane were used for temperature calibration. The former was also used for enthalpy calibration. Heat capacity calibration was performed with a PMMA standard (supplied by Acros [12]), using the heat capacity difference between two temperatures, one above and one below the glass transition temperature of PMMA, to make sure that heat capacity changes were adequately measured. Standard modulation conditions used in the experiments are an amplitude A_T of 1 °C and a period p of 60 s. Unless stated otherwise, non-isothermal experiments were performed at an underlying heating rate of 1 °C min^{-1}.

Samples were pretreated under vacuum 10 °C below the expected cloud point of the blend, prior to the introduction into hermetic aluminum crucibles. These crucibles were perforated to ensure an inert atmosphere around the sample, reducing degradation of PEO at higher temperatures.

3. Results and discussion

3.1. Phase diagram of PEO/PES

The phase diagram of PEO/PES can be constructed by means of MTDSC. Important features are illustrated for a PEO/PES (4000/20,000 g mol^{-1}) blend.

3.1.1. Glass transition and melting point for homogeneous blend

The glass transitions (T_g) of different PEO/PES blends, quenched from the miscible melt, increase with increasing PES content (Fig. 1: T_g). Fig. 2 shows T_g as calculated by the inflection point, together with the width of T_g (ΔT_g) for each blend. The fact that broader transitions are found for higher PES content (ΔT_g up to 90 °C for 20/80 PEO/PES) is in agreement with considerations of local dynamics of polymer blends [13]. This broadness of the transition means that miscibility is not attained at a molecular level, sometimes termed borderline miscibility [14].

For blends with a higher fraction of PEO (65/35, 55/45, 50/50 in Fig. 1), cold crystallization starts immediately after (partial) devitrification of the quenched blend (around −20, 13 and 37 °C, respectively), complicating the calculation of T_g and also ΔT_g. Also note that a higher crystallization rate for these blends means that the quench procedure to form a completely amorphous material is not reliable: T_g measured in the subsequent heating will not necessarily correspond to the composition of the amorphous blend. Melting of the crystalline phase occurs around 60 °C [3].

For a higher PES content (20/80 and 10/90 in Fig. 1), a decrease of the heat capacity before the endset of T_g of the homogeneous blend is noticed due to phase separation inducing partial vitrification (see also Section 3.2.1). In the phase diagram in Fig. 2, constructed with the data of Fig. 1, open symbols were used for blends for which the calculation of T_g and ΔT_g might be inaccurate.

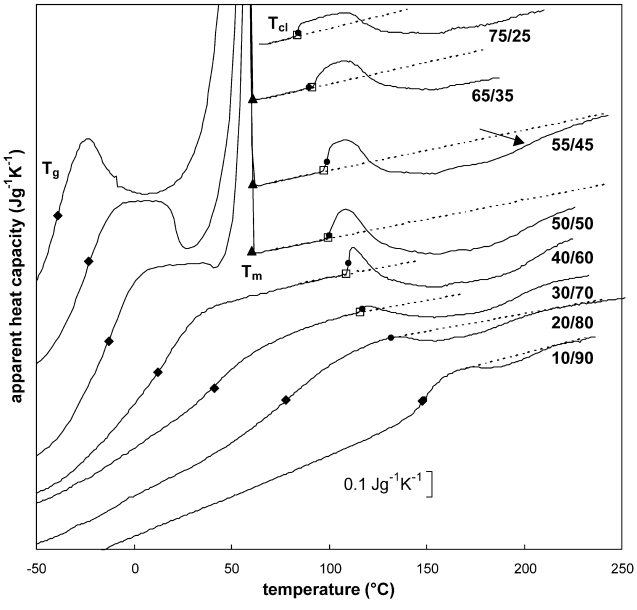

Fig. 1. T_g (◆), T_m (▲) and T_{cp} as measured by MTDSC (□) and optical microscopy (●) at 1 °C min^{-1} for different PEO/PES (4000/20,000 g mol^{-1}) blends after quenching from the homogeneous melt, linear extrapolation from the homogeneous melt (- - -).

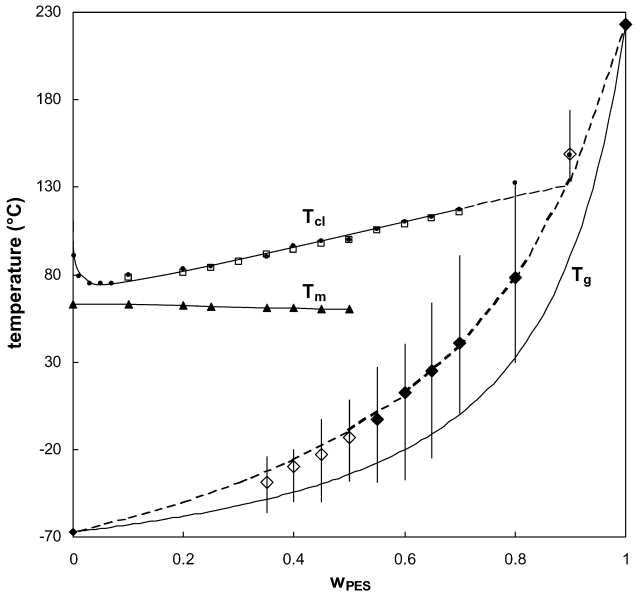

Fig. 2. Phase diagram for PEO/PES (4000/20,000 g mol^{-1}): T_g (◆ and ◇, see text), ΔT_g (vertical bars), T_m (▲), T_{cl} as measured by MTDSC (□) and optical microscopy (●), and T_g-composition relations: Couchman (—) and Gordon–Taylor with $k = 0.25$ (- - -).

In Fig. 2, the composition dependence of T_g has been simulated according to the Couchman equation [15]. The correspondence between the experimental points and the simulated T_g–w_{PES} curve (full line) is limited. This could be due to the calculation of T_g as the inflection point of a very wide glass transition. Moreover, the Couchman equation does not include interactions between the constituents of the blend. In the approach of Gordon and Taylor [16] (dashed line in Fig. 2), an adjustable parameter is included to take specific interactions into account. If only the accurately measured T_g values (Fig. 2: ◆) were used, a small value of the adjustable parameter ($k = 0.25$) was found, indicating weak interactions in the blend. Note that the full and dashed T_g–w_{PES} curves merely serve as an indication and point of reference, since ΔT_g (indicated by vertical bars in Fig. 2) and especially the endset of T_g will be important to understand the mobility-controlled demixing behavior (see also Section 3.2).

The melting points were determined as the endsets of the melting region (see T_m in Fig. 1). The values of T_m define the lower limits of the miscible melt region in the phase diagram for $w_{PES} < 0.5$.

3.1.2. Cloud point temperature

By raising the temperature of a miscible PEO/PES melt, phase separation occurs. It is characterized by an LCST at 75 °C and a composition of 97/3. As shown in Figs. 1 and 2,

the measured onset of the decrease in light transmittance (●) corresponds nicely to the onset of the apparent heat capacity evolution (□) for all compositions. Moreover, the onset of the sudden increase of C_p^{app} is nearly independent of the underlying heating rate (varied from 0.25 to 2.5 °C min^{-1} in this MTDSC study, see also Fig. 5), so that these onset values are a good approximation for the equilibrium binodal curve. The composition of the PEO/PES blend has a strong effect on the cloud point temperature (Fig. 1). Note that optical microscopy still allows the detection of the cloud point for low amounts of the minority component, whereas the heat effect and thus C_p^{excess} is less pronounced in MTDSC (see also Section 3.2.1).

With T_g, T_m and T_{cl} four regions of interest can be distinguished in the phase diagram of PEO/PES 4000/20,000 (Fig. 2): the (semi-crystalline) glassy region below the endset of T_g, the semi-crystalline region between the endset of T_g and T_m, the miscible homogeneous melt region between T_m and T_{cl} (or between the endset of T_g and T_{cl} if $w_{PES} > 0.5$) and the partially miscible region above T_{cl}. Note that these regions have been constructed using heating (or cooling) rates of 1 °C min^{-1}. The main focus in this paper will be on the latter two regions, where (re)mixing and demixing phenomena occur. The knowledge of the phase diagram will allow the interpretation of the temperature and time dependency of C_p^{app} for demixing and remixing in both non-isothermal and isothermal conditions.

3.1.3. Influence of molecular weight of PEO

Increasing the molecular weight of one of the components of a polymer blend results in a lower entropy of mixing, usually leading to a decrease in LCST. The critical point should move in the direction of the lower molecular weight component according to the simple Flory–Huggins treatment [5]. In the case of PEO/PES blends, however, large free volume contributions render the phase diagram intrinsically asymmetric and also result in a limited molecular weight dependency [17]. The small influence of the molecular weight on the cloud point curve is confirmed with MTDSC and light scattering measurements. As an example, the onset of C_p^{app} (the cloud point temperature) of a 50/50 PEO/PES blend varies less than 3 °C for a change in molecular weight of PEO from 4000 to 300,000 g mol^{-1} (see also Figs. 7 and 8). Note that also only minor differences (within 5 °C) were detected for T_g and ΔT_g of the homogeneous 50/50 blends of different molecular weights of PEO.

The kinetics of demixing and remixing, however, will largely depend on the molecular weight of the blend constituents (see Sections 3.2.5 and 3.3.3).

3.2. Kinetics of demixing

Below T_{cl}, the heat capacity of the homogeneous PEO/PES melt depends only on temperature and blend composition (C_p^{thermo}) and is independent of time and molecular weight of the constituents. By a temperature increase beyond T_{cl}, entering the partially miscible region, the continuous changes in composition by diffusion of components between the co-existing phases can be monitored in C_p^{app}. In this temperature zone of partial miscibility, up to temperatures as high as T_g of pure PES, the evolution of C_p^{app} is time-dependent and influenced by the composition of the blend and the molecular weight of the constituents.

Moreover, this temperature zone of partial miscibility can be subdivided by the temperature of intersection between the cloud point curve (T_{cl}–w_{PES}) and the evolution of the glass transition with composition (T_g–w_{PES}), enabling to distinguish a demixing zone *without* (zone I) and *with* (zone II) interference of partial vitrification.

In zone I (small 'quench depths' in the partially miscible region), the phase separating PEO-rich and PES-rich co-existing phases should reach the equilibrium compositions on the cloud point curve. At higher temperatures (zone II), however, T_g of the PES-rich phase results in strongly mobility-restricted phase separation and the equilibrium compositions are not attained [6]. Important in this respect is ΔT_g: the endset of T_g of the PES-rich phase has to be used here, since this limit marks the onset of possible interference of partial vitrification.

3.2.1. Effect of composition and partial vitrification

The composition of the PEO/PES blend has a strong effect on the evolution of C_p^{app} beyond T_{cl} and on the relative importance of zone I and zone II (Fig. 1). For the experimental conditions used, the boundary between both zones is determined by extrapolation of the heat capacity evolution of the homogeneous melt from below T_{cl} to higher temperatures (dashed line). In zone I, C_p^{app} has a higher value than the extrapolated reference due to an excess contribution (C_p^{excess}) of the endothermic heat of demixing. In zone II, a decrease of the heat capacity is observed and partial vitrification prevails. Devitrification occurs at even higher temperatures and is indicated by an arrow in Fig. 1. The upper limit of zone II corresponds with the devitrification of (almost) pure PES with a T_g value of 223 °C.

These findings of partial vitrification, induced by phase separation (while increasing the temperature), are confirmed by a dynamic rheometry experiment on the 50/50 PEO/PES blend (Fig. 3) and at the same heating rate (1 °C min^{-1}) as the MTDSC experiment in Fig. 2. At first an increasing viscous response with temperature is measured for the homogeneous melt. At 100 °C, the onset of phase separation results in a decrease in the loss angle (δ), due to the increased elastic contributions of the phase-separated morphology [18]. Two local extremes in δ are noticed around 123 and 230 °C, which are relaxation peaks associated with partial vitrification and devitrification of the PES-rich phase, respectively. In between both extremes, the storage shear modulus is at an almost constant maximum value. Dynamic rheometry is very suitable to measure these

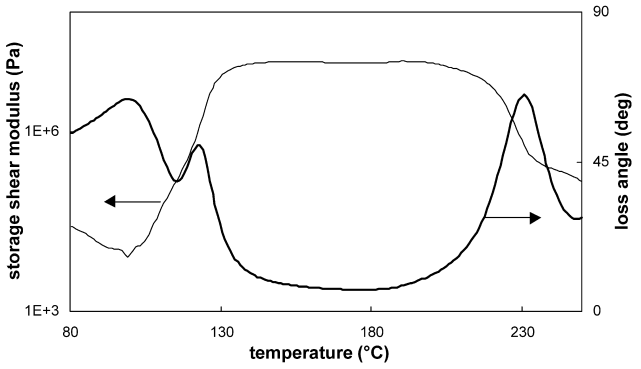

Fig. 3. Dynamic rheometry experiment at 1 °C min^{-1} and 1 Hz, showing the storage shear modulus and the loss angle for 50/50 PEO/PES (4000/20,000 g mol^{-1}).

low modulus materials (around 10^7 Pa), whereas dynamic mechanical analysis can be adopted for measuring vitrification and devitrification in blends with higher fractions of PES, exhibiting higher moduli [6].

For blends with higher amounts of PEO (55/45, 65/35 and 75/25 in Fig. 1) a lower cloud point temperature is found (Fig. 2), whereas the onset of vitrification always occurs around 120 °C. This results in broadening of zone I for higher fractions of PEO.

In the 20/80 and 10/90 PEO/PES blends, no onset of C_p^{app} can be measured, whereas light scattering still depicts a cloud point in the glass transition region of the blends. This indicates that devitrification of part of the blend directly initiates demixing. Also note that the measured cloud point lies above the extrapolated cloud point curve in Fig. 2 (dashed line). So, one should be careful in using the onset of decrease in light transmittance (cloud point) as a measure of the binodal curve and should be aware of the relative position of T_g and ΔT_g versus T_{cl} for blends of high PES content.

3.2.2. Enthalpy of demixing

If PEO/PES (4000/20,000 g mol^{-1}) is demixed at 1 °C min^{-1}, the enthalpy of demixing, calculated by means of C_p^{excess} (against the extrapolated reference line,C_p^{thermo}), is smaller than 1.8 J g^{-1} for all compositions. An asymmetric function of the weight percentage of PES is found (Fig. 4), falling to zero at higher PES percentages (Fig. 1: 20/80 and 10/90 PEO/PES). This can be ascribed to partial vitrification of the PES-rich phase following shortly after the onset of phase separation. From that moment, the competition between further phase separation and vitrification smears out the small enthalpy of demixing over a wide temperature range, so that a quantification of this heat effect by MTDSC becomes impossible. For a blend of PEO with poly(enamino nitrile) (PEAN) in which vitrification does not interfere with phase separation, a maximum for the enthalpy of demixing was found for a 50/50 blend [19].

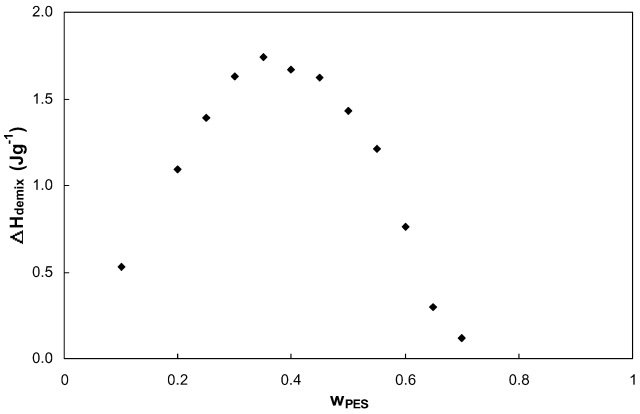

Fig. 4. Enthalpy of demixing as a function of composition for a PEO/PES (4000/20,000 g mol^{-1}) blend (calculation see text).

3.2.3. Effect of underlying heating rate

The time-dependency of the demixing process is clearly noticed in Fig. 5 by changing the underlying heating rate. At temperatures below zone I (or T_{cl}) and above zone II, the heat capacity is independent of the heating rate (C_p^{thermo}).

In zone I and II, however, the value of C_p^{app} is affected by the heating rate. By lowering the heating rate, more time is available to attain the equilibrium compositions of the co-existing phases. However, instead of getting larger, the enthalpy of demixing of zone I gets smaller due to a narrowing of zone I by an earlier interference of partial vitrification (starting at lower temperatures). This is in agreement with a more pronounced decrease in C_p^{app} and thus a more pronounced partial vitrification at lower heating rates in zone II. This confirms the time-dependency of demixing in combination with partial vitrification in this temperature domain.

3.2.4. Step-wise quasi-isothermal demixing

The kinetics of the demixing process can best be studied (quasi)-isothermally, as was already introduced in Ref. [6]. In (quasi)-isothermal conditions, C_p^{excess} reflects the magnitude

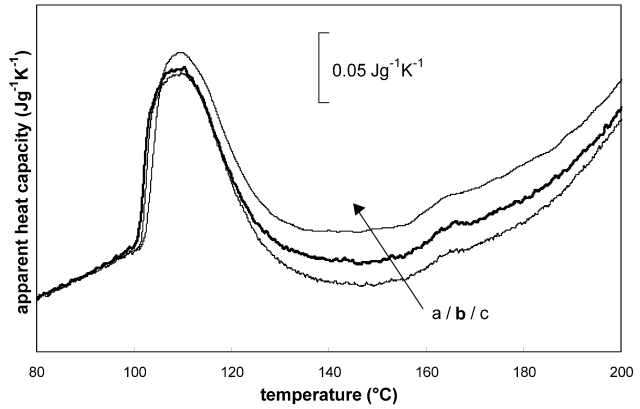

Fig. 5. Influence of the heating rate on the evolution of C_p^{app} for 50/50 PEO/PES (4000/20,000 g mol^{-1}): (a) 0.25 °C min^{-1}, (b) 0.5 °C min^{-1} and (c) 2.5 °C min^{-1}.

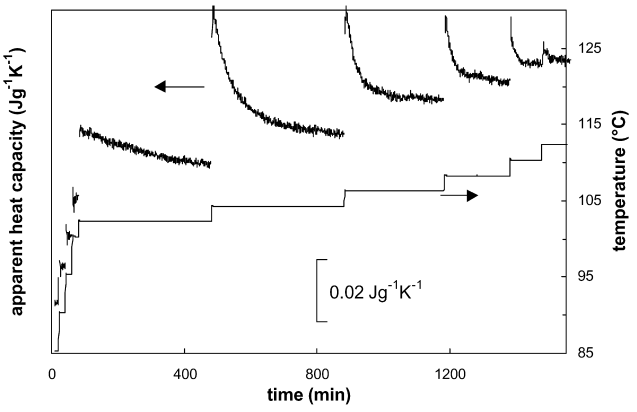

Fig. 6. C_p^{app} and corresponding temperature of a step-wise quasi-isothermal MTDSC experiment between 85 and 112 °C of 50/50 PEO/PES (4000/20,000 g mol^{-1}) with a temperature step of 2 °C beyond the cloud point ($T_{cl} = 100$ °C).

of the enthalpy of (de)mixing on the time-scale of the modulation, allowing the detection of the evolution of phase separation (irreversible process) up to a time-independent demixing/remixing equilibrium (reversible process). It is interesting to compare the value of C_p^{app} at this equilibrium state with the predicted value of C_p^{thermo} or baseline heat capacity at the same temperature.

In Fig. 6, a step-wise (quasi)-isothermal experiment is shown as a function of time for 50/50 PEO/PES (4000/20,000 g mol^{-1}). After reaching a stable value for C_p^{app} corresponding to the equilibrium state at the chosen temperature, a step-wise increase of a few degrees (e.g. 2 °C) was applied.

The same measurement is depicted in Fig. 7(a) as a function of temperature, using vertical lines for the isothermal steps and thick dots for the stable time-independent values. Below the cloud point at 100 °C no time-dependency is observed and all (quasi)-isothermal measurements coincide with C_p^{thermo} measured at 1 °C min^{-1}. Beyond T_{cl}, however, a time-dependent excess contribution is superimposed on the extrapolated baseline heat capacity (dashed line).

An evolution is seen in the equilibrium values of C_p^{app} (thick dots in Fig. 7(a)), lying also above the extrapolated baseline heat capacity. There are two possible explanations for this effect. Firstly, remixing and demixing occurring on the time scale of the modulation can result in the measured equilibrium excess contribution. When the co-existing phases of the phase-separated blend have reached the binodal compositions, the temperature modulation perturbs the equilibrium within one modulation cycle of 60 s between a more (+1 °C, demixing) or less (−1 °C, remixing) demixed state. The heat effects of demixing and remixing contribute to the amplitude of the modulated heat flow, giving rise to the time-independent excess contribution (see Section 2.4). This effect is very small: only 1% of the absolute value of the extrapolated C_p^{thermo}. A second explanation for the time-independent excess contribution is that the attained phase-separated morphology can have an effect

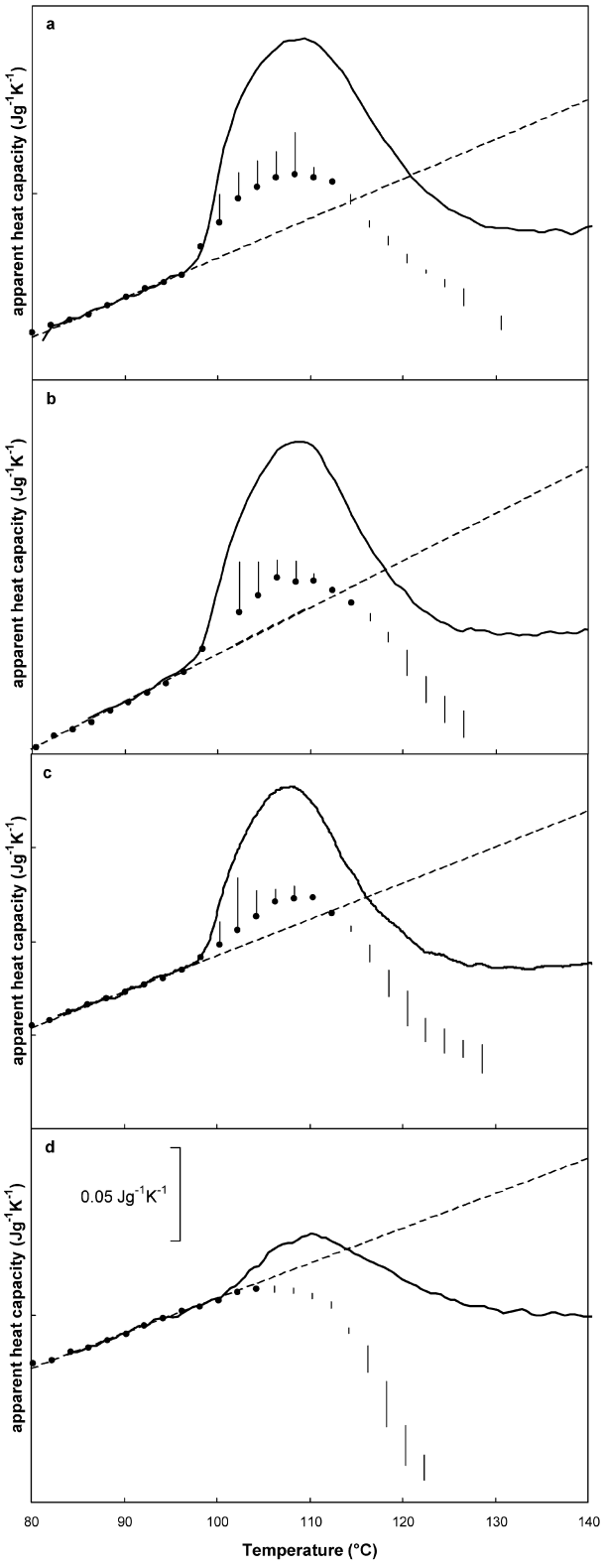

Fig. 7. C_p^{app} at 1 °C min^{-1} (full curves) for 50/50 PEO/PES blends of different M_w(PEO) superimposed on the corresponding step-wise quasi-isothermal measurements: (a) M_w(PEO) = 4000 g mol^{-1} (see also Fig. 6), (b) 8000 g mol^{-1}, (c) 20,000 g mol^{-1}, (d) 300,000 g mol^{-1}. Vertical lines indicate the evolution with time to the equilibrium value (●), if no equilibrium reached (open end), extrapolation of the baseline heat capacity (- - -).

on C_p^{thermo} of the blend. This means that a simple extrapolation of the heat capacity is not possible and effects related to the transformation from a homogeneous to a heterogeneous blend, like the break-up of specific interactions, should be taken into account.

3.2.5. Influence of molecular weight of PEO on demixing kinetics

The diffusion-controlled nature of the phase separation process leads to a clear influence of the molecular weight of the blend components on the rate of demixing. The effect of the molecular weight of PEO, ranging from 4000 to 300,000 g mol^{-1}, is depicted in Fig. 7(a)–(d) for both step-wise (quasi)-isothermal and non-isothermal demixing conditions. The evolution of the (quasi)-isothermal equilibrium C_p^{app} (thick dots) is shown in comparison to the extrapolated baseline heat capacity (dashed lines) and C_p^{app} in non-isothermal conditions (full curves). The slower kinetics of demixing for higher molecular weights of PEO result in smaller heat effects on the time-scale of the modulation (beyond T_{cl} in zone I) and thus in a smaller value of C_p^{excess}. This influence of molecular weight also holds for the equilibrium value, in favor of the interpretation that a time-independent excess contribution remains due to an equilibrium of demixing and remixing heat effects.

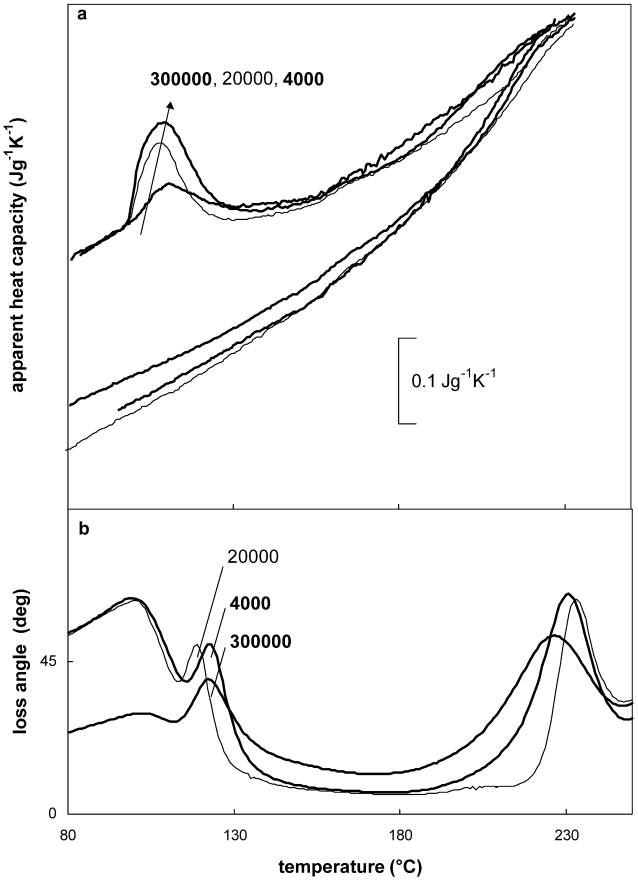

Fig. 8. Influence of M_w(PEO) on the evolution of C_p^{app}, and loss angle from dynamic rheometry for 50/50 PEO/PES (M_w(PES) = 20,000 g mol^{-1}): M_w(PEO) = 4000, 20,000 and 300,000 g mol^{-1}; both heating and cooling at 1 °C min^{-1} are shown for C_p^{app}.

As already pointed out in Section 3.2.1, partial vitrification results in a decrease in C_p^{app} in zone II. In the step-wise measurements of Fig. 7(a)–(c), the interference of partial vitrification is noticed around 115 °C for M_w(PEO) of 4000, 8000 and 20,000 g mol^{-1}, whereas this interference starts at least 10 °C lower for M_w(PEO) of 300,000 g mol^{-1} (Fig. 7(d)). This is probably the result of a higher T_g and ΔT_g of the PES-rich phase for the highest molecular weight of PEO, for the same PEO/PES ratio (see Section 3.1.3).

Note that for the step-wise (quasi)-isothermal experiments in zone II a stable state was not reached within the isothermal time-scales needed in zone I (the vertical lines of Fig. 7(a)–(d) do not end in thick dots in zone II), pointing out the slowly proceeding phase separation restricted by the partial vitrification of the high-T_g PES-rich phase.

In contrast with the interpretation of the step-wise (quasi)-isothermal experiments of Fig. 7(a)–(d), the effect of molecular weight on the demixing kinetics in non-isothermal demixing conditions (Fig. 8(a) and full curves in Fig. 7(a)–(d)) is not straightforward. For blends with higher molecular weight of PEO, the slower demixing kinetics will give rise to co-existing phases with compositions that are further away from the equilibrium binodal compositions. As a consequence, smaller enthalpies of demixing are calculated in zone I and a delayed degree of partial vitrification is observed (zone II). In comparison to step-wise (quasi)-isothermal demixing, the onset of partial vitrification is most delayed in the case of M_w(PEO) of 300,000 g mol^{-1}.

The combined effects of molecular weight and a constant heating rate are further illustrated in Fig. 8(b), showing dynamic rheometry experiments at 1 °C min^{-1}. The 300,000 g mol^{-1} PEO sample first shows a more elastic response in the homogeneous melt region, a smaller decrease in δ at the onset of phase separation around 100 °C, and a less pronounced and less constant elastic response by partial vitrification of the high-T_g PES-rich phase in between the two local relaxation maxima around 120 and 230 °C. A more gradual devitrification of the PES-rich phase is observed for M_w(PEO) of 300,000 g mol^{-1}. Note that an interesting comparison can be made with MTDSC measurements of curing (thermosetting) systems, in which T_g increases by chemical reactions. Partial vitrification and devitrification is interfering with cure kinetics as a combined effect of the rate of T_g-increase and the heating rate [9].

A subsequent cooling experiment at 1 °C min^{-1} (only shown in Fig. 8(a) for C_p^{app}) depicts a slightly higher T_g for the PES-rich phase than during heating (devitrification), meaning that further phase separation occurs beyond 210 °C. The endset of this T_g coincides with the one of pure PES. The ΔT_g, however, is 13 °C higher for the blend system, indicating a remaining influence of PEO in the PES-rich phase. The difference in the composition of the

co-existing phases between the heating (more PEO in PES-rich phase) and the subsequent cooling (less PEO in PES-rich phase) is nicely illustrated by the lower heat capacities at the same temperature in the latter.

3.3. Kinetics of remixing

Fig. 8(a) indicates that all 50/50 PEO/PES blends are still partially vitrified after cooling from 230 to 80 °C. It means that the kinetics of remixing do not allow to attain the homogeneous equilibrium state during the cooling at 1 °C min^{-1}. It has already been shown [6] for a 75/25 PEO/PES (17,000/61,000 g mol^{-1}) blend that if partial vitrification occurs during demixing (zone II), devitrification of the high-T_g phase is necessary to attain the thermodynamically stable remixed state, leading to very long remixing times of up to 4000 min. Only if vitrification during demixing is absent (zone I), remixing is almost instantaneous.

3.3.1. Effect of demixing temperature (zone I or II) on non-isothermal remixing

In Fig. 9 two non-isothermal remixing experiments starting from different demixing temperatures are compared by (i) heating 50/50 PEO/PES (4000/20,000 g mol^{-1}) at 1 °C min^{-1} from the miscible melt region to a demixing temperature of 115 °C (zone I) or 138 °C (zone II), respectively, and after a certain demixing time (ii) cooling at 1 °C min^{-1} to a temperature in the miscible melt region. Non-isothermal remixing from zone I clearly shows an excess contribution in C_p^{app} (Fig. 9, curve b). Complete remixing occurs in the miscible melt region (60–100 °C), since T_{cl} and the evolution of C_p^{app} in a second heating coincide with the first heating (not shown). Non-isothermal remixing from zone II shows a totally different evolution, due to the interference of partial vitrification in the demixing step (Fig. 9, curve c). The PES-rich phase vitrifies more during cooling, seen as a further decrease in C_p^{app}. No clear excess contribution is seen here, since the vitrified PES-rich phase is unable to contribute to remixing and the co-existing PEO-rich phase contains almost pure PEO according to the phase diagram of Fig. 2. Only a small bump below 100 °C is noticed, probably due to a competition between a thermodynamically driven tendency to remix (accompanied by devitrification) and vitrification controlled by the cooling rate. A non-equilibrium condition is reached in the miscible melt region and a long isothermal remixing step is needed to re-establish equilibrium.

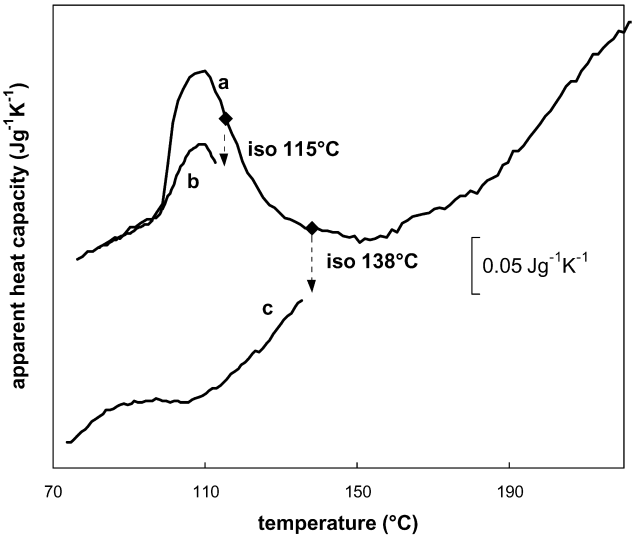

Fig. 9. Overlay of C_p^{app} of 50/50 PEO/PES (4000/20,000 g mol^{-1}): (a) heating at 1 °C min^{-1} to 220 °C, (b) cooling at 1 °C min^{-1} after demixing for 600 min at 115 °C (in zone I), (c) cooling at 1 °C min^{-1} after demixing for 300 min at 138 °C (in zone II); the point at which the isothermal step was inserted has been indicated (◆).

3.3.2. Quasi-isothermal remixing: influence of remixing temperature

Quasi-isothermal devitrification is an ideal probe for studying the slow remixing process after demixing in zone II, as shown in Fig. 10 for 50/50 PEO/PES (4000/20,000 g mol^{-1}). The influence of the remixing temperature is analyzed at 70, 80 and 90 °C in the miscible melt region after demixing for 300 min at 138 °C. The remixing process takes more time at lower temperatures (more than 2000 min at 70 °C), which can be ascribed to lower diffusion coefficients in combination with the fact that the PES-rich phase is further vitrified at lower temperatures, as seen in Fig. 9. Note that the heat capacity evolutions in Fig. 10 do not attain the same final level due to the effect of temperature on C_p^{thermo} in the miscible melt region.

3.3.3. Quasi-isothermal remixing: influence of molecular weight of PEO

Remixing at 90 °C, after demixing at 138 °C for 300 min, is compared for 50/50 PEO/PES blends of different

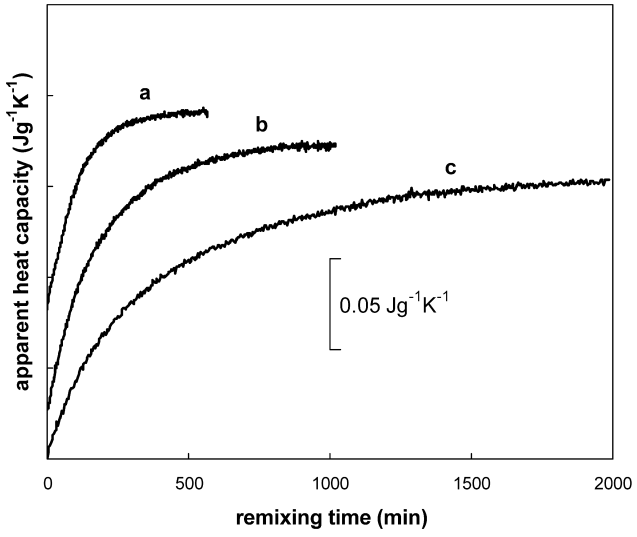

Fig. 10. Quasi-isothermal remixing at (a) 90, (b) 80 and (c) 70 °C of 50/50 PEO/PES (4000/20,000 g mol^{-1}), after demixing for 300 min at 138 °C (zone II).

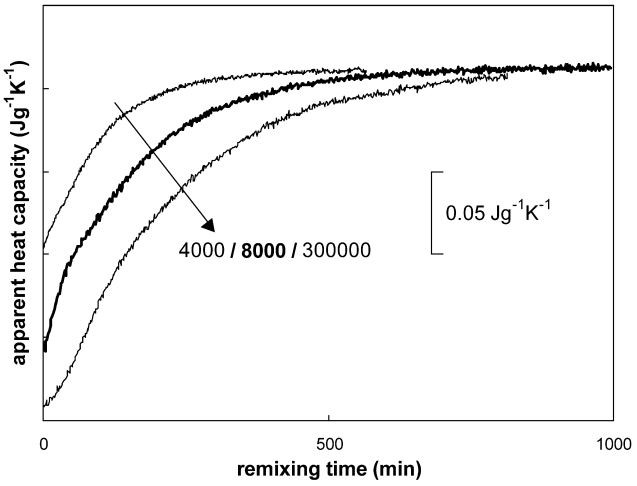

Fig. 11. Quasi-isothermal remixing at 90 °C of 50/50 PEO/PES with M_w(PEO) = 4000, 8000 and 300,000 g mol^{-1}, after demixing for 300 min at 138 °C (zone II).

M_w(PEO) in Fig. 11. In none of the blends an equilibrium state is attained during the demixing step. For higher M_w(PEO), slower demixing at 138 °C is expected due to lower diffusion rates, resulting in a smaller increase of T_g for the PES-rich phase over the same demixing time (300 min). However, as concluded from the step-wise quasi-isothermal experiments on the blend with M_w(PEO) of 300,000 g mol^{-1}, slightly higher T_g and ΔT_g values for the same composition results in a higher degree of partial vitrification over longer isothermal time scales (see Section 3.2.5). These compensating effects lead for all blends of different molecular weight to almost the same decrease in C_p^{app} at 138 °C due to partial vitrification (not shown). The high-T_g PES-rich phase formed at 138 °C is further frozen in upon cooling (Fig. 9, curve c). The same remixing temperature (90 °C) is permitted for comparison, since only a minor effect of molecular weight on T_{cl} is seen (see Section 3.1.3, Figs. 7 and 8). In Fig. 11, the decreasing rate of remixing with increasing M_w(PEO) is clearly shown, caused by slower diffusion between the co-existing phases. After remixing, C_p^{thermo} of the respective homogeneous blends is attained again.

4. Conclusions

MTDSC is a powerful tool for the real-time study of transformations in partially miscible polymer blends, such as PEO/PES showing LCST demixing with an interference of partial vitrification. Not only the determination of T_{cl}, but also of T_g and T_m of the homogeneous blend are important to understand the demixing behavior of this blend. The position of T_g and especially ΔT_g in relation to T_{cl} determine two zones in the phase diagram of PEO/PES: zone I corresponding to the region in which most of the endothermic enthalpy of demixing is found and zone II in which partial vitrification effects prevail. A very useful output signal, resulting from the sinusoidal perturbation in MTDSC, is the (modulus of the complex) heat capacity. It is called 'apparent heat capacity' in this case, since excess contributions by heat effects of demixing and remixing on the time-scale of the modulation are retrieved in this signal. Since noise and baseline effects turn up in the non-reversing heat flow and not in the former signal, small heat effects related to phase separation in polymer blends can still be measured (less than 2 J g^{-1} for PEO/PES). Moreover, the (apparent) heat capacity can also be measured quasi-isothermally, allowing the real-time study of the kinetics of demixing (above T_{cl}) and remixing (between T_g or T_m and T_{cl}) in isothermal conditions for different blend compositions and molecular weights of the components.

A higher fraction of the high-T_g component PES results in slower kinetics due to mobility restrictions. Partial vitrification decreases the rate of demixing and remixing. Increasing the molecular weight of PEO results in a decreased diffusion rate between the co-existing phases too.

In step-wise quasi-isothermal measurements an equilibrium excess contribution is noticed in zone I of the phase diagram. This effect, probably due to demixing and remixing heat effects on the time-scale of the modulation, decreases for higher M_w(PEO) and is typically smaller than 1% of the baseline heat capacity. Future work consists of looking at systems with larger specific interactions, in which changes in the MTDSC modulation parameters (amplitude and period) should further clarify the physical meaning of the excess contribution. Phase separation in polymer–solvent systems will also be considered in this respect.

The methodology developed in this paper for temperature-induced phase separation is applicable to all kinds of partially miscible polymer systems and will also be extended to reaction-induced phase separation [20,21].

Acknowledgements

The work of S. Swier was supported by grants of the Flemish Institute for the Promotion of Scientific-Technological Research in Industry (I.W.T.). The work of R. Pieters was supported by grants of the Research Council (O.Z.R.) of the Free University of Brussels (V.U.B.).

References

[1] Dreezen G, Ivanov DA, Nysten B, Groeninckx G. Polymer 2000;41:1395.
[2] Walsh D, Singh V. Makromol Chem 1984;185:1979.
[3] Dreezen G, Fang Z, Groeninckx G. Polymer 1999;40:5907.
[4] Dreezen G, Mischenko N, Koch MHJ, Reynaers H, Groeninckx G. Macromolecules 1999;32:4015.
[5] MacKnight WJ, Karasz FE. Polymer blends. In: Allen G, Bevington JC, editors. Comprehensive polymer science, Polymer characterization, vol. 1. Oxford: Pergamon Press, 1989. p. 113–30.

[6] Dreezen G, Groeninckx G, Swier S, Van Mele B. Polymer 2001;42:1449.
[7] Reading M, Luget A, Wilson R. Thermochim Acta 1994;238:295.
[8] Wunderlich B, Jin Y, Boller A. Thermochim Acta 1994;238:277.
[9] Van Assche G, Van Hemelrijck A, Rahier H, Van Mele B. Thermochim Acta 1997;304/305:317.
[10] De Meuter P, Amelrijckx J, Rahier H, Van Mele B. J Polym Sci Part B: Polym Phys 1999;37:2881.
[11] Varma-Nair M, Wunderlich B. J Phys Chem Ref Data 1980;20:349.
[12] Gaur U, Wunderlich B. J Phys Chem Ref Data 1982;11:313.
[13] Lodge TP, McLeish TCB. Macromolecules 2000;33:5278.
[14] Mandal TK, Woo EM. Polymer 1999;40:2813.
[15] Couchman PR, Karasz FE. Macromolecules 1978;11:117.
[16] Gordon M, Taylor JS. J Appl Chem 1952;2:493.
[17] Walsh D, Rostami S, Singh VB. Makromol Chem 1985;186:145.
[18] Vinckier I, Laun HM. Rheol Acta 1999;38:274.
[19] Moore JA, Kim JH. Macromolecules 1992;25:1427.
[20] Swier S, Van Assche G, Van Hemelrijck A, Rahier H, Verdonck E, Van Mele B. J Thermal Anal 1998;54:585.
[21] Swier S, Van Mele B. Thermochim Acta 1999;330:175.